ISSN 1330-3651 (Print), ISSN 1848-6339 (Online) https://doi.org/10.17559/TV-20220803122813
Original scientific paper

# Analysis of the Influence of the Number of Burnishing Passes on the Geometric Structure of Aluminium Composites Surface

Paweł KAROLCZAK*, Mite TOMOV

**Abstract:** The paper presents the results of burnishing tests of composites based on AlSi9Mg aluminum alloy matrix, reinforced with Saffil ceramic fibers and silicon carbide particles. The tested material was produced at the Wroclaw University of Science and Technology. The tested materials were turned and then ball burnished. After each subsequent burnishing pass, the surfaces were measured by contact and the roughness parameters were calculated. It has been found that it is possible to obtain the *Sa* roughness of composites thanks to burnishing at the level of 0.1 μm. The paper shows that for each material there is an optimal and limit number of passes, which guarantees the lowest roughness for a fiber-reinforced composite these are 4 passes, and for a composite reinforced with SiC particles 5 passes. The research showed that the reduction of the roughness peaks of composites after burnishing is definitely greater than that of the valleys. The research presented in the article broadens the knowledge of aluminum composites burnishing.

**Keywords:** aluminium composites; burnishing; geometric structure; measurements; surface roughness

## 1 INTRODUCTION

Modern constructions require materials that have not only excellent mechanical properties, but also other, in many cases, specific features. Additionally, it is often required that the material of construction has a low density to keep the structure light. Composites are such materials. Their base material may be polymers (thermosetting or thermoplastic polymers), light metal alloys, ceramics, etc. The reinforcement that gives mechanical properties is most often ceramics in the form of fibers or particles [1]. Wood is a separate material group. It is classified as a composite and is called a natural composite. Wood is processed using methods similar to metal composites [2].

Composite materials are widely used in means of transport, construction, military, and medicine. The widening use of these materials is often limited due to their complexity and high costs related to the wear of cutting tools, as well as the difficulty in obtaining satisfactory product quality, especially surface roughness [1, 3, 4]. Tools such as polycrystalline diamond, cubic boron nitride, and tungsten carbide are suggested to reduce blade wear. Many research results show that with the use of polycrystalline diamond or cubic boron nitride blades, a surface with a lower roughness can be obtained then after the use of carbide blades [1, 3-5]. Unfortunately, these tools are very expensive and their use is not always possible for economic reasons. The alternative to traditional methods are unconventional treatments such as Electrical Discharge Machining (EDM), Laser Beam Machining (LBM), Abrasive Water Jet Machining (AWJM), Electro Chemical Machining (ECM), Electro Chemical Discharge Machining (ECDM) [6]. They are used to shape elements made of both polymer and metal composites. Each of these methods is characterized by the fact that the material is removed using energy different than mechanical. In addition, the tools in these methods are definitely cheaper than cutting blades, and their wear is not a big cost. Unconventional methods, despite their clear advantage in the form of low tool costs, do not guarantee the quality of the machined surface. The main problem in the EDM process is the deposition of the resolidified layer, which deteriorates the surface quality [7]. During LBM laser processing, the excessive amount of laser heat is responsible for the melting and evaporation of the matrix and reinforced particles, causing a chemical reaction and transforming the microstructure of the matrix material [8]. In AWJM, material removal occurs through erosion, not deformation wear [9]. The quality of the treated surface is largely dependent on the differences in the size of the abrasive and reinforcement particles. Pitting can occur on the surface during the ECM, especially at low voltages because of the low current density. Furthermore, at low electrolyte flow rate, unfavorable streaks may appear on the treated surface [6]. Another technique used in the processing of composites, which replaces, for example, drilling, can be punching [10].

Good surface quality is guaranteed by conventional machining processes such as turning and milling. Unfortunately, they also leave unevenness on the surface resulting from the kinematic-geometric impact of the blade on the surface or vibrations of the machine tool. These irregularities increase friction between the two elements during assembly and thus increase wear and shorten the service life of the machined element [11]. To overcome these problems, conventional finishing processes such as grinding, honing, and lapping are used. However, it should be remembered that when the matrix of the composite is a light, soft aluminum alloy, these processes are difficult to implement because the soft matrix clogs the pores of the abrasive tool. As a result, it is difficult to remove microcavities that can scratch the machined surface. Burnishing can be used instead of traditional finishing methods. The burnishing process reduces surface defects and modifies the microstructure of the treated surface. Burnishing takes place both on flat surfaces and on the inner and outer surfaces of cylindrical elements. The main applications of burnishing processes are in the aerospace and automotive industries.

Research is being conducted on the influence of burnishing on the surface quality of materials that make up the matrix of composites, as well as the composite materials themselves. They apply to both rolling and sliding burnishing. Cagan et al. investigated the possibilities of improving the surface of a workpiece made of Al 7075-T6 by ball burnishing [12]. It was observed that

the surface quality of the Al alloy improved as a result of the increase in force and the number of passes and the reduction of the feed. The optimal number of passes was found to be 4. Thorat et al. conducted similar research, however, on the aluminum alloy 6061 [13]. Based on Gray Relational Analysis, they found that minimizing roughness and maximizing hardness is also possible with 4 burnishing passes. Boozarpoor et al. investigated the possibility of burnishing the 6061-T6 multi-roll aluminum alloy [14].It was found that the amount of feed rate had the greatest influence on the surface roughness. The number of rolls was classified as the second important parameter. This number can be considered as the number of burnishing passes. The analysis of variance carried out showed that 6 burnishing rollers should be selected to achieve the minimum surface roughness. Kurkute et al. burnished in their research aluminum alloy 63400 [15]. It was found that the most important parameter influencing surface roughness is feed, while the increase in microhardness is most influenced by the force and the number of tool passes. Additionally, harder metals that can form the matrix of composites can be burnished.An example is the research presented in [16]. Maheshwari et al. put through a test of burnishing titanium alloys. It was found that the best surface finish can be obtained with the number of passes 3. Czechowski et al. compared the degree of surface roughness reduction and increase in microhardness of the aluminum alloy EN AW-AlCu4MgSi (A) and aluminum composites as a result of the use of sliding burnishing [17]. For the EN AW-AlCu4MgSi (A) alloy, the value of the coarseness reduction coefficient KRa was greater than 10, while for composites with an aluminum alloy matrix it ranged from 6 to 8. Varga and Ferencsik presented an interesting conclusion [18]. They found that the number of burnishing passes of the aluminum alloy positively influenced the surface hardness, but was of little importance for the residual compressive stresses measured in the surface layer.

Aluminum matrix composites (AMC) have been burnished in various tests. Nestler and Schubert studied an aluminum composite reinforced with SiC particles. The experimental results presented in [19] show that the AMC sliding burnishing leads to a significant reduction of the surface roughness value and filling the voids on the surface. An interesting conclusion from the research is shown in [20]. During burnishing of a particle-reinforced aluminum composite with a feed rate greater than 0.05 mm, the surface structure exhibits roughness corresponding to the theoreticalcalculated roughness values. Furthermore, the burnishing process causes strong compressive residual stresses in the aluminum matrix, and the absolute values of the residual stresses in the axial direction are much higher than the absolute values of the residual stresses in the circumferential direction. A separate group of composite materials is those based on polymers. Research is also conducted on the possibility of improving surface quality by burnishing. For example, Denkena et al. found that the burnishing ball has a positive effect on the surface integrity of the material [21]. The tribological improvement is attributed to the pressure exerted by the ball on the surface, which causes the peaks to deform plastically down the valleys, resulting in a much smoother surface [22]. As in the case of metal composites, the parameters of theburnishing process, i.e., the burnishing force, the burnishing speed, the burnishing feed rate, and the number of passes affect the finish of the finished element [23, 24]. Carbon fiber reinforced polymers (CFRP) were burnished by Cagan et al. [25]. The best *Ra* was achieved after four burnishing runs. The *Ra* value did not show much variation in the first three passes; however, in the fourth pass, a significant reduction in this parameter was observed.

The analysis of the literature shows that composites with durable and hard reinforcements are not as susceptible to burnishing as their matrix. However, it is difficult to determine what number of burnishing passes is optimal and guarantees the lowest or specified roughness. It is related with a wide variety of industrial composites. The study covered two composites, the production method of which was developed at the Wroclaw University of Science and Technology. This research broadens the knowledge of the machinability of composites as a whole group of materials, but also of these two specific materials

## 2 EXPERIMENTAL PROCEDURE

Three light materials were tested, an aluminum composite material reinforced with alumina Saffil ceramic fibers ($Al_2O_3$) and an aluminum composite material reinforced with silicon carbide (SiC) particles. Fiber and particle content by volume was 10%. The third reference material was the unreinforced composite matrix, i.e. the EN AC-43330 alloy (AlSi9Mg). Tab. 1 to Tab. 4 contain information on the chemical composition and selected properties of the matrix, as well as Saffil fibres used.

**Table 1** Chemical composition (% weight) of alloy Aluminum EN AC-43330 (AlSi9Mg)

| Al | Si | Cu | Mg | Mn | Fe | Ti | Zn |
|---|---|---|---|---|---|---|---|
| rest | 9,5 | < 0,05 | 0,35 | < 0.1 | < 0,18 | 0,15 | 0,07 |

**Table 2** Properties of Aluminum EN AC-43330 (AlSi9Mg)

| Density / gm/cm$^3$ | Tensile Strength, Yield / MPa | Tensile Strength, Ultimate / MPa |
|---|---|---|
| 2.5 | 210 - 230 | 6.9 |
| Young's Modulus / GPa | | Brinell Hardness |
| 71 | | 91 - 94 |

**Table 3** Chemical composition of Saffil fiber

| $Al_2O_3$ | $SiO_2$ | Fe, Cr, Ni, Na, Mg, Ca, chlorides |
|---|---|---|
| 96 - 97% | 3 - 4% | Trace amounts |

**Table 4** Properties of Saffil fiber

| Density / g/cm$^3$ | Tensile Strength / GPa | Compressive Strength / GPa |
|---|---|---|
| 3.3 | 1.8 | 6.9 |
| Young's Modulus / GPa | Rigidity Modulus / GPa | Durable up to temperature / $^0$C |
| 300 | 122 | 1600 |

The properties of the composite reinforced with Saffil fibers differ from those of the matrix. The AlSi9Mg alloy has a hardness in the range of 74 - 80 HB. When reinforced with fibers, the composite is much harder than it the values are in the range of 106 - 124 HB, depending on the filtration pressure used during its production. Tensile strength also increases by 20% for this compound. This composite is also characterized by a lower value of the thermal expansion coefficient as a function of temperature than the unreinforced matrix. When reinforcement is used in the form of silicon carbide particles, the strength properties are

increased, and we are dealing with a higher abrasion resistance in relation to the matrix. There is a 40% increase in hardness compared to the matrix itself. As the composite reinforces with SiC particles, the thermal conductivity and the thermal expansion coefficient are reduced.

The entrance surfaces to the burnishing process have been prepared by turning. Both turning and burnishing were performed on a TUR 50S universal lathe. On the basis of preliminary tests, the parameters of turning and burnishing were selected. The feed rate $f$ = 0.08 mm/rev and the cutting speed $v_c$ = 83 m/min were used. The turning depth was 0.5 mm. 7 pressing passes were made, each with a depth of 0.05 mm. Burnishing was carried out with a diamond ball (Fig. 1). The study conditions are summarized in Tab. 5.

**Table 5** Summary of Experimental Conditions

| | |
|---|---|
| Work pieces | Aluminum alloy AlSi9Mg<br>Composite Al/$Al_2O_3$ fibres<br>Composite Al/SiC particles |
| Machine | TUR 50 S lathe |
| Burnishing type | Ball pressure burnishing |
| Turning and burnishing speed / m/min | 83 |
| Feed rate / mm/rev | 0,08 |
| Number of burnishing passes | 7 |

Roughness measurements were carried out with the SURFTEST SV-3200 profilographometer (Fig. 1) with a measuring range in the $X$ axis 100 mm, a tip pitch of 800 µm, with additional equipment in the form of a positioning table in the $Y$ axis, allowing the 3D surface topography to be obtained. The device had a measuring tip in the form of a diamond needle with a cone rounding radius of 2 µm and a cone angle of 60°. The profilographometer used has built-in software for roughness testing FORMTRACEPACK and 3D McCube Ultimate surface analysis.

When measuring the 3D surface, an area of 0.5 mm by 0.5 mm was scanned. The measurement step with the $X$ and $Y$ axes was 5 µm. 10000 points were registered in this way. The measured surfaces were subjected to a procedure including: separating a 0.45 × 0.45 mm fragment from the measured surface (in order to eliminate possible measurement errors at the border of the tested area), leveling the surface using the least squares method, removing the shape outline by means of a second degree polynomial, and signal filtering (separation of waviness profile from roughness). Roughness from waviness was separated with a Gaussian filter. The limiting wavelength $\lambda_c$ for the Gaussian filter was 250 µm.

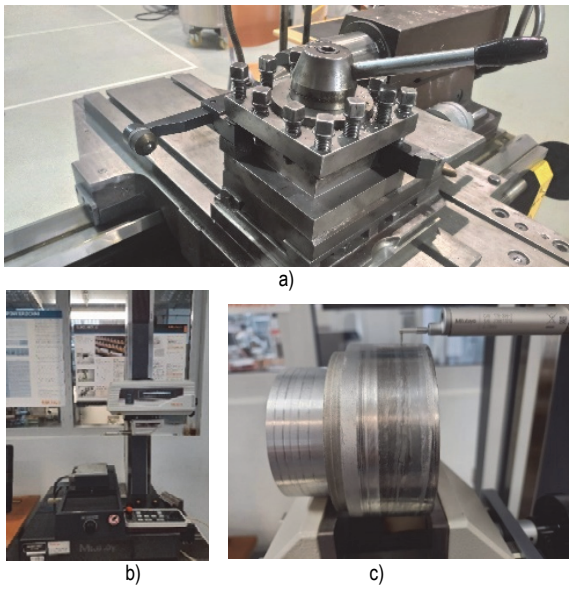

a) b) c)

**Figure 1** Ball burner clamped in the lathe tool post (a); Mitutoyo SV-3200 profilographometer (b), measuring tip and burnished sample (c)

## 3 TEST RESULTS AND DISCUSSION

Tab. 6 to Tab. 8 show the results of surface roughness measurements of the tested materials after turning and subsequent burnishing passes. Two average parameters were selected for the analysis, i.e. the most popular and most commonly used in industry, *Sa*, and the mean square deviation of the surface from the mean line, i.e. *Sq*. The second group of parameters were the height parameters, i.e. the greatest roughness of the *Sz* surface and the greatest elevation *Sp* and the greatest depression *Sv*. The analysis was supplemented by skewness (*Ssk*) and kurtosis (*Sku*) classified as statistical parameters and the fractal box dimension classified as additional parameters.

**Table 6** The results of surface roughness measurements of the aluminum alloy, which is the matrix of the composite, after turning and subsequent burnishing passes

| | *Sa* / µm | *Sq* / µm | *Sz* / µm | *Sp* / µm | *Sv* / µm | *Ssk* / - | *Sku* / - | *Df* / - |
|---|---|---|---|---|---|---|---|---|
| turning | 1,3 | 1,63 | 11,9 | 5,63 | 6,24 | 0,08 | 3,28 | 2,56 |
| 1 burnishing pass | 1,25 | 1,55 | 10,7 | 5,43 | 5,23 | 0,03 | 2,78 | 2,55 |
| 2 burnishing passes | 2,33 | 2,83 | 18,1 | 7,11 | 10,99 | −0,25 | 2,69 | 2,47 |
| 3 burnishing passes | 1,12 | 1,46 | 13 | 4,84 | 8,11 | −0,93 | 4,51 | 2,37 |
| 4 burnishing passes | 0,31 | 0,52 | 6,27 | 1,36 | 4,91 | −2,9 | 18,9 | 2,55 |
| 5 burnishing passes | 0,1 | 0,14 | 1,71 | 0,44 | 1,27 | −2,15 | 15,6 | 2,5 |
| 6 burnishing passes | 0,24 | 0,47 | 7,46 | 1,29 | 6,17 | −3,26 | 23,7 | 2,28 |
| 7 burnishing passes | 0,3 | 0,42 | 4,57 | 2,63 | 1,95 | 0,51 | 6,94 | 2,6 |

**Table 7** The results of surface roughness measurements of the composite Al / $Al_2O_3$ fibers after turning and subsequent burnishing passes

| | *Sa* / µm | *Sq* / µm | *Sz* / µm | *Sp* / µm | *Sv* / µm | *Ssk* / - | *Sku* / - | *Df* / - |
|---|---|---|---|---|---|---|---|---|
| turning | 0,38 | 0,54 | 3,99 | 1,53 | 2,46 | −0,87 | 5,76 | 2,62 |
| 1 burnishing pass | 0,42 | 0,55 | 4,31 | 1,75 | 2,55 | −0,54 | 4,08 | 2,75 |
| 2 burnishing passes | 0,27 | 0,35 | 3,67 | 1,15 | 2,51 | −0,6 | 5,14 | 2,68 |
| 3 burnishing passes | 0,25 | 0,31 | 3,63 | 1,47 | 2,16 | −0,63 | 4,96 | 2,59 |
| 4 burnishing passes | 0,12 | 0,17 | 2,84 | 0,85 | 1,99 | −2,36 | 20,8 | 2,58 |
| 5 burnishing passes | 0,17 | 0,25 | 3,26 | 0,91 | 2,35 | −2,08 | 13 | 2,65 |
| 6 burnishing passes | 0,14 | 0,21 | 2,86 | 0,66 | 2,19 | −2,6 | 18,1 | 2,62 |
| 7 burnishing passes | 0,11 | 0,14 | 1,33 | 0,49 | 0,84 | −0,29 | 3,43 | 2,83 |

**Table 8** The results of surface roughness measurements of the composite Al /SiC particles after turning and subsequent burnishing passes

| | *Sa* / µm | *Sq* / µm | *Sz* / µm | *Sp* / µm | *Sv* / µm | *Ssk* / - | *Sku* / - | *Df* / - |
|---|---|---|---|---|---|---|---|---|
| turning | 1,9 | 2,41 | 17,5 | 8,59 | 8,88 | 0,03 | 3,2 | 2,46 |
| 1 burnishing pass | 2,23 | 2,78 | 20,3 | 10,4 | 9,83 | 0,04 | 3,01 | 2,32 |
| 2 burnishing passes | 0,64 | 1,09 | 12,2 | 4,24 | 8,01 | −1,87 | 11,6 | 2,25 |
| 3 burnishing passes | 0,21 | 0,31 | 4,41 | 2,21 | 2,2 | −1,3 | 9,65 | 2,49 |
| 4 burnishing passes | 0,28 | 0,41 | 6,5 | 1,22 | 5,27 | −2,04 | 16,6 | 2,26 |
| 5 burnishing passes | 0,19 | 0,29 | 3,65 | 1,49 | 2,16 | 0,42 | 8,23 | 2,44 |
| 6 burnishing passes | 0,22 | 0,38 | 6,66 | 1,32 | 5,34 | −4,72 | 47,4 | 2,63 |
| 7 burnishing passes | 0,29 | 0,45 | 6,27 | 3,2 | 3,07 | −1,74 | 11,3 | 2,6 |

When analyzing the data contained in Tab. 6 to Tab. 8, one should notice, first of all, the significantly lower values of the *Sa* and *Sz* parameters after turning the fiber-reinforced composite than the particle-reinforced composite. This result is the effect of different reinforcement decohesion mechanisms. In the case of fibers, they are sheared by a blade and shredded into smaller pieces or pulled to a lesser extent from the warp to the surface. The particles, on the other hand, are most often pulled out of the matrix, resulting in the formation of craters on the surface, which increase the surface roughness. Secondly, as expected, the surface roughness of both the composites and the matrix itself is reduced as a result of burnishing.

As the surfaces prepared for the burnishing process had such divergent roughness, it was decided that the burnishing effectiveness, in the case of average and height parameters, will be defined as the reduction factors for the given parameters (Eq. 1):

$$K_{sx} = \frac{Sx}{Sx'} \tag{1}$$

where: *Sx'* value of a given roughness parameter after burnishing, *Sx* value of a given roughness parameter before burnishing (after turning).

The analysis of the influence of successive burnishing passes on the surface roughness of the tested materials was divided into parts. The analyzed roughness parameters were grouped so as to describe similar surface features. Fig. 2 and Fig. 3 show the values of the coefficient *KSa* and *KSq* for the roughness reduction *Sa* and *Sq*.

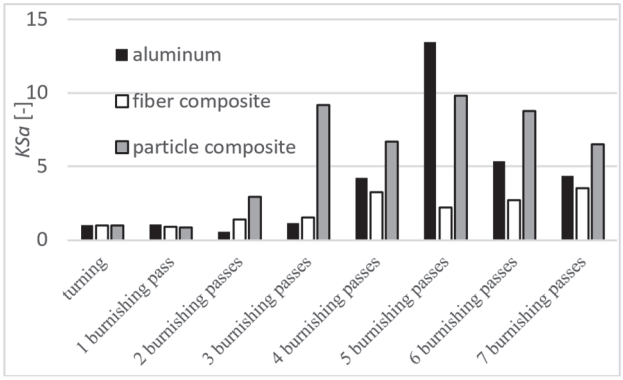


**Figure 2** *KSa* coefficient, reduction of roughness *Sa* after successive burnishing passes

By analyzing the calculated coefficients, it can be concluded that each of the tested materials reacted differently to subsequent burnishing passes. The aluminum alloy, which is the matrix for the third burnishing passes, does not show a significant decrease in the values of the average parameters. Moreover, after the second burnishing pass, a twofold increase in the values of the *Sa* and *Sq* parameters was found. Sudden and significant reductions in these parameters were observed after the fourth and fifth passes. Especially, the fifth pass improves the roughness a 13 - fold reduction of the *Sa* parameter and a 12 - fold reduction of the *Sq* parameter were found. The next pass deteriorates the roughness to a certain extent, while the 7 pass improves the roughness again. The images of the surface presented in Fig. 4 are the confirmation.

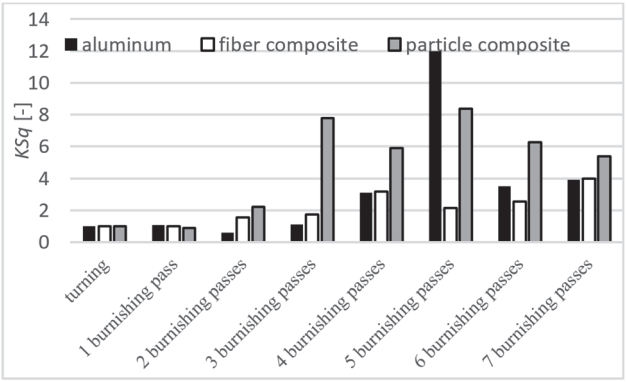


**Figure 3** *KSq* coefficient, reduction of roughness *Sq* after successive burnishing passes

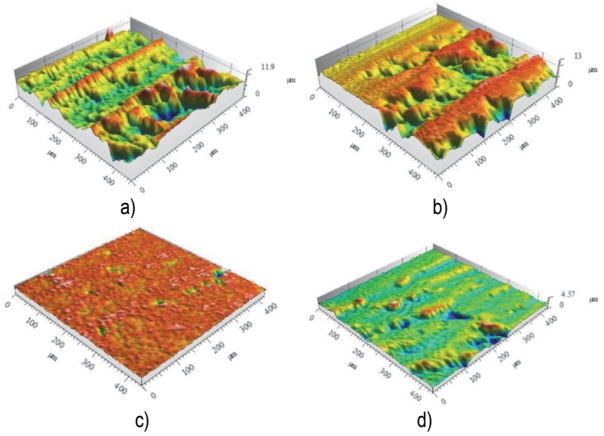


**Figure 4** Surfaces of the AlSi9Mg aluminum alloy after turning (a), after the third (b), fifth (c) and seventh (d) burnishing passes

During burnishing of the composite reinforced with Saffil fibers, a similar trend of changes in Sa and Sq parameters up to the third pass was observed as for the matrix. Despite the very different input surfaces after turning, in the case of both materials, a slight increase in the values of these parameters after the first pass and a significant decrease in their values after the next two were observed. Subsequently, the two materials react differently to burnishing. A significant increase in the values of the coefficients *KSa* and *KSq* for the composite reinforced with Saffil fibers was observed after the fourth burnishing, 3,26

and 3,19; respectively. After two more passes of the diamond ball, the roughness deteriorates. After the last test, the seventh, another decrease in the values of *Sa* and *Sq* was obtained. *KSa* and *KSq* take the values 3,5 and 3,98. These relationships are clearly visible in the surface images (Fig. 5).

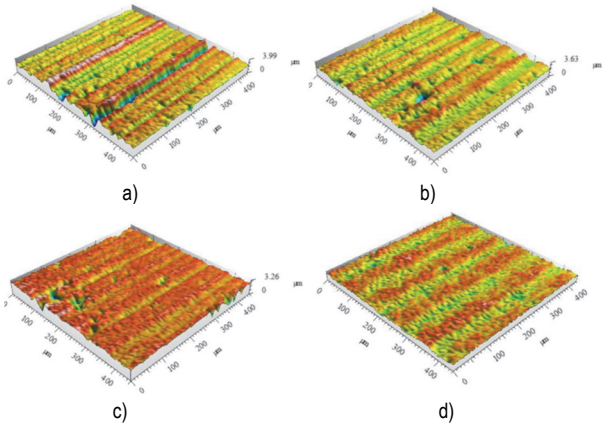


**Figure 5** Surfaces of the aluminum composite reinforced with Saffil fibres after turning (a), after the third (b), fifth (c) and seventh (d) burnishing passes

In the case of a composite reinforced with SiC particles, a reduction in the *Sa* parameter was obtained at the level of 9,17 and the *Sq* parameter at the level of 7,8 after the third pass of the diamond ball. Subsequent burnishing resulted in a slight increase in the value of these parameters, and after passing number 5, the greatest reduction was obtained in relation to the input surface after turning. *KSa* and *KSq* were values of 9,79 and 8,36, respectively. The next two burnishing passes did not bring about another improvement in smoothness and a slight increase in the values of the *Sa* and*Sq* parameters (Fig. 6).

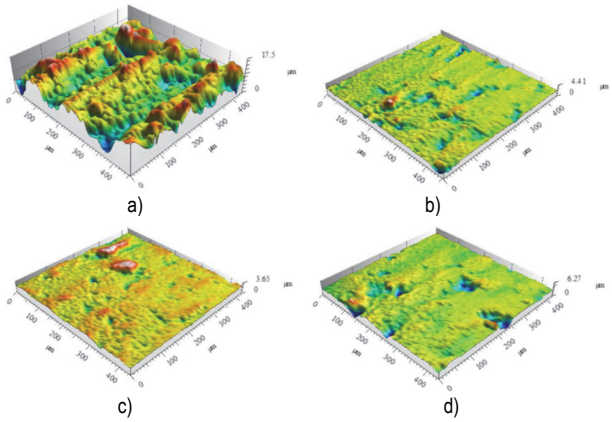


**Figure 6** Surfaces of the aluminum matrix composite reinforced with SiC particles after turning (a), after the third (b), fifth (c) and seventh (d) burnishing passes

In summarizing the analysis of the average parameters, it is worth noting that for the matrix itself and the fiber reinforced composite, regardless of the roughness of the input surface after turning, it is possible to obtain a surface with a roughness of *Sa* at a level of 0,1 µm after burnishing. Particle-reinforced composite seems to be a more difficult material to process. First, the decohesion of the particles made it more difficult to obtain a low roughness after turning, and after burnishing it was possible to reduce the *Sa* value only to 0,19 µm. During burnishing of this material, it is possible to remove whole groups of reinforcing molecules, causing the formation of craters on the surface (Fig. 6d). For each of the materials, a different number of burnishing passes was found, allowing the greatest reduction in surface roughness. For the matrix and the particle-reinforced composite, it was 5 passes, and for the composite with fibres 4 or 7. Comparing these results with literature data, it can be seen that this number is higher in [12, 13] for aluminum it was found that 4 passes give the lowest roughness, and for a harder and less plastic material these are 3 burnishing passes [16].

Another parameter analyzed was *Sz*. As a parameter that shows the highest roughness in the examined area, it is very sensitive to single peaks and depressions. As individual defects can be observed on burnished surfaces, the *KSz* coefficients of reduction of the *Sz* parameter do not reach such high values as the *KSa* and *KSq* coefficients (Fig. 7). As in the analysis of mean parameters, it can be concluded that the best quality of the matrix surface is obtained after the fifth burnishing pass, the *KSz* value is 6,96. A similar effect of the number of burnishing passes was observed for the composite reinforced with SiC particles. Here, however, the *KSz* coefficient does not exceed 5. The surface of the fiber composite has the lowest value of *Sz* after passing number 7. For this composite, after subsequent burnishing passes, the fluctuations in the values of the *Sz* parameter are the smallest.

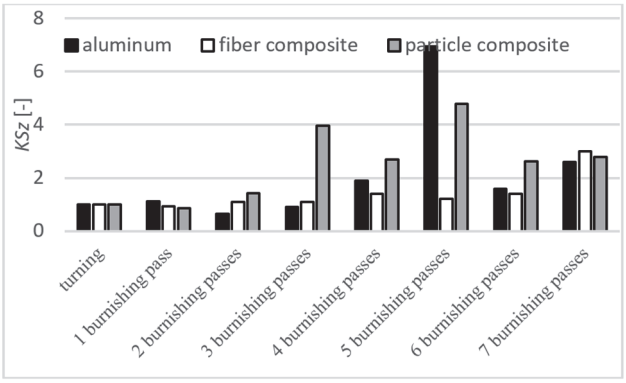


**Figure 7** *KSz* coefficient, reduction of roughness *Sa* after successive burnishing passes

Significantly lower values of the KSz coefficient than the KSa and KSq coefficients may be the result of inaccurate kneading and removing roughness peaks or the lack of the filling any cavities and valleys of roughness with the burnished and deformed material. It should also be remembered of the possibility of removing the reinforcement particles of the composite from the surface layer or crushing fragments of fibers. When the *Sp* and *Sv* parameters are analyzed, being components of the *Sz* parameter, as well as the values of the *KSp* and *KSv* coefficients, it can be assumed that during burnishing of both the aluminum matrix itself and aluminum composites, reduction of roughness peaks dominates. The reduction coefficients for the *Sp* parameter describing just the peaks have maximum values of 12,85 for the fifth pass burnishing of the matrix, and 7,04 for the SiC-reinforced composite and 3,14 for the Saffil-reinforced composite. These values are higher than in the case of the *KSv* that describes the reduction of roughness valleys. After the fifth pass of the AlSi9Mg burnishing, the *KSv* value is 4,9; which is almost

three times lower than the *KSp* (Fig. 8). For composites, this tendency is maintained, but the differences between *Kp* and *KSv* are smaller (Fig. 10 and Fig. 12).

Fig. 9 shows two surfaces after burnishing the composite matrix, for which different ratios of the *KSp* and *KSv* coefficients were observed. Both surfaces have similar values of the parameter *Sz*. However, the surface after 1 burnishing pass (Fig. 9a) is characterized by high roughness peaks and, at the same time, significant depressions. After this transition, the effect of the burnishing tool on the roughness peaks is not observed. In addition, it can be assumed that a part of the deformed material remains on the surface as a scrap and at the same time increases the value of the *Sp* parameter. After the fourth burnishing pass (Fig. 9b), no peaks are observed that have already been smoothed. On the surface, however, deep depressions are visible, significantly increasing the *Sv* parameter and at the same time reducing the *KSv* factor.

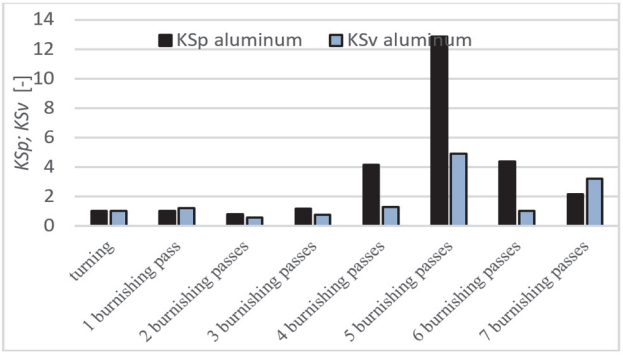


**Figure 8** *KSp* and *KSv* coefficients, reduction of the roughness *Sp* and *Sv* after successive burnishing passes of the composite matrix

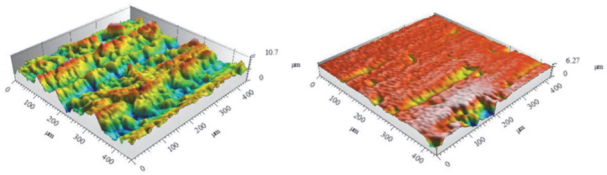


**Figure 9** AlSi9Mg alloy surface after the first (a) and fourth (b) burnishing pass

Despite the much lower roughness of *Sa* and *Sz* after turning and burnishing the fiber composite, compared to the matrix surface, the ratios of *KSp* to *KSv* after the first and fourth pass of the diamond ball are at a similar level for both materials (Fig. 8 and Fig. 10). Surfaces also have similar characteristics. After the first burnishing pass of the fiber composite, the geometric structure of the surface characteristic for turning is still retained, with the roughness peaks clearly visible (Fig. 11a). After the fourth pass, single deep depressions and no peaks are visible. These depressions may be the result of fiber decohesion or exposed voids at the fiber-matrix interface.

Fig. 12 shows the values of the coefficients of reduction of the roughness parameters *Sp* and *Sv* for the burnished composite reinforced with SiC particles. As in the case of other tested materials, the reduction of the *Sp* parameter after the fourth, fifth and sixth passes of the diamond ball is much greater than the reduction of the Sv parameter. The ratio of *KSp* to *KSv* exceeds 4 for pass number 4. This is confirmed by the surface images (Fig. 13). As a result of burnishing, the roughness peaks and as a result the directional-periodic structure characteristic for turning disappear in the subsequent passes. It can be concluded that the periodic valleys formed by rolling are also deformed. Only a few pits remain, the position of which is random (Fig. 13b).

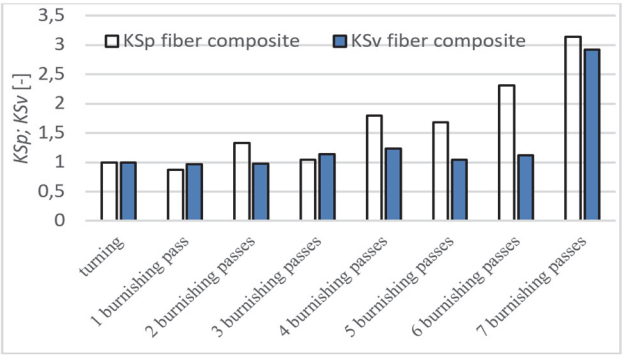


**Figure 10** *KSp* and *KSv* coefficients, reduction of the roughness *Sp* and *Sv* after successive burnishing passes of the composite reinforced with Saffil fibres

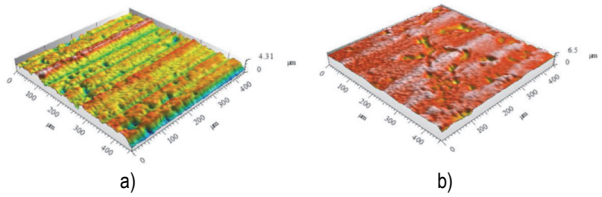


**Figure 11** Aluminum matrix composite reinforced with Saffil fibres surface after the first (a) and fourth (b) burnishing pass

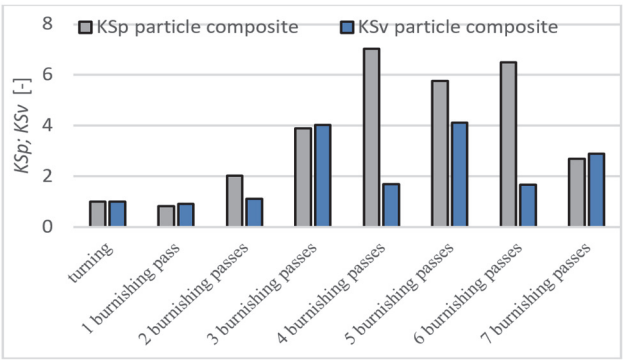


**Figure 12** *KSp* and *KSv* coefficients, reduction of the roughness *Sp* and *Sv* after successive burnishing passes of the composite reinforced with SiC particles

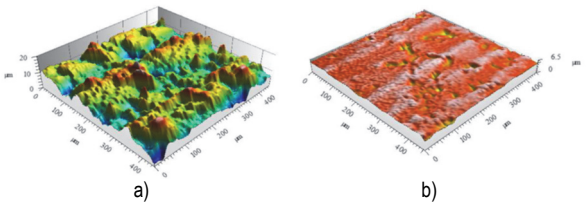


**Figure 13** Aluminum matrix composite reinforced with SiC particles surface after the first (a) and fourth (b) burnishing pass

Looking for confirmation for the visible in isometric images of surfaces, and during the analysis of the values of the parameters *Sz*, *Sp*, and *Sv* of the full crushing of the roughness peaks and the remaining certain number of the depression, the statistical, dimensionless roughness parameter *Ssk* was analyzed. This parameter is the profile asymmetry coefficient; in other words, it determines the skewness of the ordinate distribution. It has an averaging character and may be positive for structures characterized by numerous peaks or negative for surfaces dominated by

pits. The more this parameter moves away from zero, the more heterogeneous the material distribution.

As shown in Fig. 14, after turning the particle-reinforced composite and the matrix itself, it takes values close to zero, and for a fiber composite around −1. For all materials, this parameter becomes negative up to the sixth burnishing pass and moves further and further away from zero. The exception is the surface of the Al/SiCp composite after passing number 5. *Ssk* unexpectedly takes a positive value. Undoubtedly, there is the effect of visible sticking or fines of machined material on the surface (Fig. 6c). After the seventh burnishing pass, the values of the *SSk* parameter increase. This is due to the reappearance of tops formed during the burnishing itself.

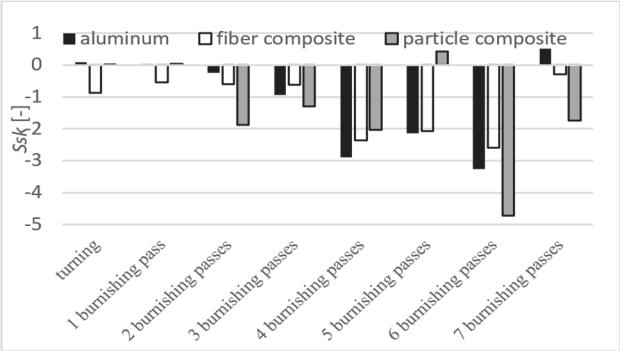


**Figure 14** The value of the *Ssk* parameter after turning and subsequent burnishing passes

Fig. 15 shows the values of the *Sku* parameter. It is a measure of the amplitude density curve's acuteness, also referred to as a flattening coefficient. The limit is adopted for *Sku* = 3, where below it the inequalities have a greater length and the vertices are more filled with material, while above it they become sharper and shorter. It follows from the definition that, because during burnishing the hard ball acts on the peaks to the greatest extent and kneads them, the *Sku* should increase with successive burnishing passes.

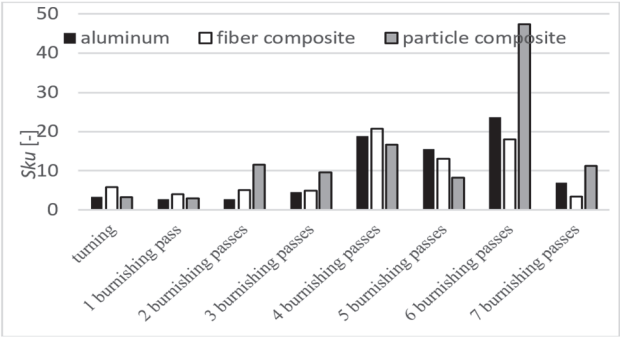


**Figure 15** The value of the *Sku* parameter after turning and subsequent burnishing passes

Fig. 15 confirms this. *Sku* grows from the first to the fourth pass for each material. In the fifth pass, it slightly reduces its value and increases again after the sixth burnout pass. As in the *Sa* or *Sz*, after the seventh pass, all trends in changes in the geometric structure of the surface are disturbed; *Sku* significantly decreases compared to the sixth pass. The maximum *Sku* values measured are 23,7 for the matrix, 20,8 for the fibrous composite, and as much as 47,4 for the particle-reinforced composite. It should be noted that the maximum *Sku* values correlate with the minimum *Ssk* values for each of the tested materials. Fig. 16 shows the surfaces after the sixth burnishing pass, where the *Ssk* and *Sku* values are extreme, show a clear lack of peaks on these surfaces, and those that can be distinguished are flattened without sharp ends.

An additional study was to determine the effect of burnishing passes on the value of the box fractal dimension of the surface. The idea of determining this dimension is simple and consists of applying to the measured structure a regular grid with components of a constant size. Depending on the research dimension (2D/3D), the elements take the form of squares or cubes, "boxes" of constant size ε. Then it is calculated how many of the components are present in the measured N structure ($\varepsilon$). This process is repeated for the smaller ε size and the plot ln ($N$ ($\varepsilon$))/ln($\varepsilon$) is plotted. In the McCube Ultimate software, in which the calculations were performed, the method called closing boxes is used. It consists of covering each section of the profile with a box of width $\varepsilon$ (in points) and calculating the volume $V\varepsilon$ of all boxes covering the entire surface. This procedure is repeated with boxes of different widths to build the plot ln ($V\varepsilon$)/ln($\varepsilon$). The fractal dimension is calculated from the slope of the regression line. Fig. 17 shows a diagram of the changes in box size after successive burnishing passes. It is clearly visible that for most surfaces it has the highest values for the fibrous composite and the lowest values for the composite reinforced with particles. With successive passes of the burnishing ball, the values of this dimension change. However, no relationship can be shown between this dimension and the number of burnishing passes. It seems advisable to check the correlation between the box fractal dimension and the standard roughness parameters. Such a study brings many interesting conclusions, also in composite surfaces [26].

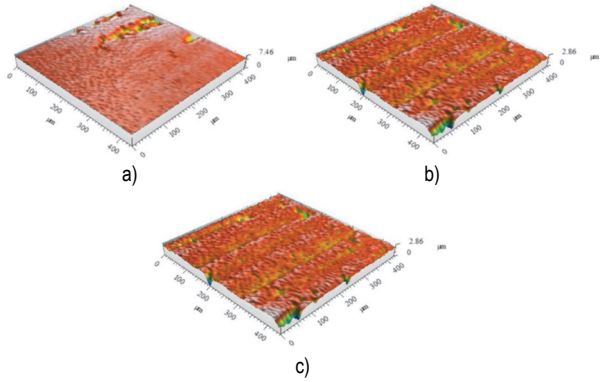


**Figure 16** Surfaces after the sixth burnishing pass: aluminum matrix (a); fiber-reinforced composite (b); composite reinforced with SiC particles (c)

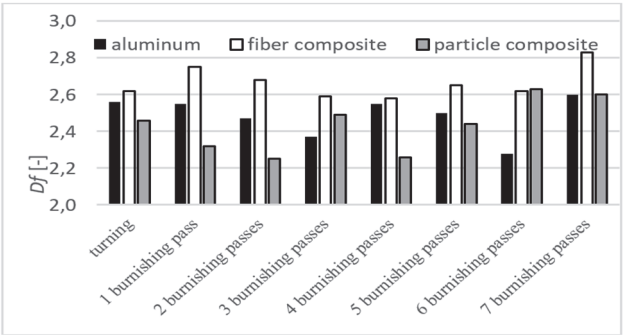


**Figure 17** Value of the box fractal dimension after turning and subsequent burnishing passes

## 4 CONCLUSIONS

Based on the research, it was found that:
- after aluminum composites burnishing, it is possible to obtain a surface of good quality described by the *Sa* parameter with a value of 0.1 μm,
- appropriate selection of the number of burnishing passes allows to obtain a specific required roughness above the minimum possible,
- there is a limit number of burnishing passes, beyond which the surface roughness no longer improves, and the surface quality deteriorates,
- in the case of the matrix itself and the composite reinforced with particles, the greatest reduction in the roughness parameters *Sa* and *Sq* was observed after the fifth burnishing pass, for the Saffil-reinforced composite these were the fourth and seventh passes,
- the greatest reduction in surface roughness occurs after burnishing the matrix, in the case of harder composites, the reduction is not so large,
- during burnishing, mainly roughness peaks are reduced - the *KSp* coefficients reach much higher values than the *KSv* for all tested materials,
- along with successive burnishing transitions, the values of the box fractal dimension of the surface change their values; however, a clear relationship between this dimension and the number of passes cannot be determined,
- in order to fully assess the surface after burnishing, also other roughness parameters than *Sa* and *Sz* should be analyzed.

## 5 REFERENCES


[1] Das, M., Mishra, D., & Mahapatra, T. R. (2019). Machinability of metal matrix composites. *Materials Today: Proceedings*, *18*, 5373-5381. https://doi.org/10.1016/j.matpr.2019.07.564

[2] Vasilko, K. & Murčinková, Z. (2019). Machining of Wood as a Natural Composite Material. *Tehnički vjesnik*, *26* (2), 363-367. https://doi.org/10.17559/TV-20171110183526

[3] Bhardwaj Ajay, R., Vaidya, A. M., & Shekhawat, S. P. (2020). Machining of Aluminium Metal Matrix Composite. *Materials Today: Proceedings*, *21*, 1396-1402. https://doi.org/10.1016/j.matpr.2020.01.179

[4] Deshmukh, S. P., Shrivastava, R., & Thakar, C. M. (2022). Machining of composite materials through advance machining process. *Materials Today: Proceedings*, *52*(3), 1078-1081. https://doi.org/10.1016/j.matpr.2021.10.495

[5] Karolczak, P., Kołodziej, M., & Kowalski, M. (2020). Effectiveness of diamond blades in the turning of aluminium composites. *Advances in Science and Technology. Research Journal*, *14*(4), 262-272. https://doi.org/10.12913/22998624/127436

[6] Kumari, B. M., Dixit, A. R., & Ashis, M. (2017). Studies on Non-traditional Machining of Metal Matrix Composites. *Materials Today: Proceedings*, *4*, 8226-8239. https://doi.org/10.1016/j.matpr.2017.07.165

[7] Dinesh, K. S., Ravichandran, M., Alagarsamy, S. V., Meignanamoorthy, M., & Sakthivelu, S. (2020). Effect of EDM process parameters on material removal rate and surface roughness of metal matrix composites. *Materials Today: Proceedings*, *21*(1), 616-618. https://doi.org/10.1016/j.matpr.2019.06.725

[8] Pramanik, A. (2014). Developments in the non-traditional machining of particle reinforced metal matrix composites. *International Journal of Machine Tools and Manufacture*, *86*, 44-61. https://doi.org/10.1016/j.ijmachtools.2014.07.003

[9] Shanmugam, D. K., Chen, F. L., Siores, E., & Brandt, M. (2002). Comparative study of jetting machining technologies over laser machining technology for cutting composite materials. *Composite Structures*, *57*(1-4), 289-296. https://doi.org/10.1016/S0263-8223(02)00096-X

[10] Ceritbinmez, F. & Yapici A. (2021). An Investigation of Punching the MWCNTs Doped Composite Plates by Using Different Cutting Profiles. *Tehnički vjesnik*, *28* (2), 385-390. https://doi.org/10.17559/TV-20191026222142

[11] Grzesik, W. & Żak, K. (2012). Modification of surface finish produced by hard turning using superfinishing and burnishing operations. *Journal of Materials Processing Technology*, *212*(1), 315-322. https://doi.org/10.1016/j.jmatprotec.2011.09.017

[12] Cagan, S. C. & Buldum, B. B. (2019). Effects of ball burnishing on the surface quality of Al 7075 alloy. *Materials Testing*, *61*(11), 1105-1108. https://doi.org/10.3139/120.111428

[13] Thorat, S. R. & Thakur, A. G. (2018). Optimization of burnishing parameters by taguchi based GRA method of AA 6061 aluminum alloy. *Materials Today: Proceedings*, *5*(2), 7394-7403. https://doi.org/10.1016/j.matpr.2017.11.410

[14] Boozarpoor, M. & Teimouri, R. (2021). Parametric study of multi-roller rotary burnishing process. *International Journal of Lightweight Materials and Manufacture*, *4*(2), 179-194. https://doi.org/10.1016/j.ijlmm.2020.10.001

[15] Kurkute, V. & Chavan, S. T. (2018). Modeling and Optimization of surface roughness and microhardness for roller burnishing process using response surface methodology for Aluminum 63400 alloy. *Procedia Manufacturing*, *20*, 542-547. https://doi.org/10.1016/j.promfg.2018.02.081

[16] Maheshwari, A. S. & Gawande, R. R. (2017). Influence of specially designed high-stiffness ball burnishing tool on surface quality of titanium alloy. *Materials Today: Proceedings*, *4*(2), 1405-1413. https://doi.org/10.1016/j.matpr.2017.01.162

[17] Czechowski, K. & Toboła, D. (2017). Slide finishing burnishing of metal alloys and metal matrix composites. *Mechanik*, *90*(7), 552-554. https://doi.org/10.17814/mechanik.2017.7.70

[18] Varga, G. & Ferencsik, V. (2022). Investigation of the Effect of Surface Burnishing on Stress Condition and Hardening Phenomena. *Tehnički vjesnik*, *29* (4), 1247-1253. https://doi.org/10.17559/TV-20211110171854

[19] Nestler, A. & Schubert, A. (2015). Effect of machining parameters on surface properties in slide diamond burnishing of aluminium matrix composites. *Materials Today: Proceedings*, *2*, S156-S161. https://doi.org/10.1016/j.matpr.2015.05.033

[20] Nestler, A. & Schubert, A. (2018). Roller burnishing of particle reinforced aluminium matrixcomposites. *Metals*, *8*(2), 95. https://doi.org/10.3390/met8020095

[21] Denkena, B., Grove, T., & Maiss, O. (2017). Surface texturing of rolling elements by hard ball-end milling and burnishing. *The International Journal of Advanced Manufacturing Technology*, *93*(9), 3713-3721. https://doi.org/10.1007/s00170-017-0809-9

[22] Janczewski, Ł., Toboła, D., Brostow, W., Czechowski, K., Lobland, H. E. H., Kot, M., & Zagorski, K. (2016). Effects of ball burnishing on surface properties of low density polyethylene. *Tribology International*, *93*, 36-42. https://doi.org/10.1016/j.triboint.2015.09.006

[23] Nguyen, T. T. & Le, X. B. (2018). Optimization of interior roller burnishing process for improving surface quality. *Materials and Manufacturing Processes*, *33*(11), 1233-1241. https://doi.org/10.1080/10426914.2018.1453159

[24] Grzesik, W. & Żak, K. (2014). Characterization of surface integrity produced by sequential dry hard turning and ball

burnishing operations. *Journal of Manufacturing Science and Engineering*, *136*(3). https://doi.org/10.1115/1.4026936

[25] Cagan, S. C., Buldum, B. B., & Ozkul, I. (2019). Experimental investigation on the ball burnishing of carbon fiber reinforced polymer. *Materials and Manufacturing Processes*, *34*(9), 1062-1067. https://doi.org/10.1080/10426914.2019.1615078

[26] Karolczak, P., Kowalski, M., & Raszka, K. (2021). Assessment of the Possibility of Using Fractal Analysis to Describe the Surface Aluminum Composites after Turning. *Advances in Science and Technology. Research Journal*, *15*(4), 49-60. https://doi.org/10.12913/22998624/141935

**Contact information:**

**Paweł KAROLCZAK**, PhD Eng.
(Corresponding author)
Faculty of Mechanical Engineering,
Wrocław University of Science and Technology,
Ignacego Łukasiewicza 5, 50-371 Wrocław, Poland
E-mail: pawel.karolczak@pwr.edu.pl

**Mite TOMOV**, PhD, Associate professor
Faculty of Mechanical Engineering-Skopje,
Ss Cyril end Methodius" University in Skopje,
Karpos II, 1000 Skopje, North Macedonia